

of the shape boundary points are assumed to be known. This limits the proposed approach to those applications where the segmentation of the shape image is unstable or unavailable. Second, the metric selection is critical, and the discriminability highly depends on the properties of the metric. If the metric is sensitive to shape topology such as inner-distance, the methods may cause some problems. For example, occlusion may cause the topology of shapes to change, and in such cases MDM will surely have a degrading performance due to the disadvantages of the metric. Third, MDM is data-independent while the dimensionality reduction used is data-dependent, so the proposed approach may be limited in shape recognition applications. At last, though we only tested the proposed method on two leaf shape datasets, the MDM approach could be applied to other shape recognition tasks involving single closed contours. How to extend MDM to capture the features of an open curve or a multi-contour shape is our future research focus.

REFERENCES

- [1] D. Zhang and G. Lu, "Review of shape representation and description techniques," *Pattern Recognit.*, vol. 37, no. 1, pp. 1–19, Jan. 2004.
- [2] S. Belongie, J. Malik, and J. Puzicha, "Shape matching and object recognition using shape context," *IEEE Trans. Pattern Anal. Mach. Intell.*, vol. 24, no. 4, pp. 509–522, Apr. 2002.
- [3] E. G. M. Petrakis, A. Diplaros, and E. Milios, "Matching and retrieval of distorted and occluded shapes using dynamic programming," *IEEE Trans. Pattern Anal. Mach. Intell.*, vol. 24, no. 11, pp. 1501–1516, Nov. 2002.
- [4] P. N. Belhumeur, D. Chen, S. Feiner, D. W. Jacobs, W. J. Kress, H. Ling, I. Lopez, R. Ramamoorthi, S. Sheorey, S. White, and L. Zhang, "Searching the world's herbaria: A system for visual identification of plant species," in *Proc. Eur. Conf. Comput. Vis.*, vol. 4, 2008, pp. 116–129.
- [5] G. McNeill and S. Vijayakumar, "2D shape classification and retrieval," in *Proc. Int. Joint Conf. Artif. Intell.*, Edinburgh, U.K., 2005, pp. 235–242.
- [6] G. McNeill and S. Vijayakumar, "Hierarchical procrustes matching for shape retrieval," in *Proc. IEEE Conf. Comput. Vis. Pattern Recognit.*, Jun. 2006, pp. 885–894.
- [7] C. Scott and R. Nowak, "Robust contour matching via the order preserving assignment problem," *IEEE Trans. Image Process.*, vol. 15, no. 7, pp. 1831–1838, Jul. 2006.
- [8] A. M. Bronstein, M. M. Bronstein, A. M. Bruckstein, and R. Kimmel, "Analysis of two-dimensional non-rigid shapes," *Int. J. Comput. Vis.*, vol. 78, no. 1, pp. 67–88, Jun. 2008.
- [9] P. F. Felzenszwalb and J. D. Schwartz, "Hierarchical matching of deformable shapes," in *Proc. IEEE Conf. Comput. Vis. Pattern Recognit.*, Minneapolis, MN, Jun. 2007, pp. 1–8.
- [10] H. Ling and D. W. Jacobs, "Shape classification using the inner-distance," *IEEE Trans. Pattern Anal. Mach. Intell.*, vol. 29, no. 2, pp. 286–299, Feb. 2007.
- [11] H. E. A. El Munim and A. A. Farag, "Shape representation and registration using vector distance functions," in *Proc. IEEE Conf. Comput. Vis. Pattern Recognit.*, Minneapolis, MN, Jun. 2007, pp. 1–8.
- [12] M. Daliri and V. Torre, "Robust symbolic representation for shape recognition and retrieval," *Pattern Recognit.*, vol. 41, no. 5, pp. 1799–1815, May 2008.
- [13] C. Xu, J. Liu, and X. Tang, "2D shape matching by contour flexibility," *IEEE Trans. Pattern Anal. Mach. Intell.*, vol. 31, no. 1, pp. 180–186, Jan. 2009.
- [14] L. J. Latecki, R. Lakaemper, and U. Eckhardt, "Shape descriptors for non-rigid shapes with a single closed contour," in *Proc. IEEE Conf. Comput. Vis. Pattern Recognit.*, Hilton Head, SC, Jun. 2000, pp. 424–429.
- [15] T. Adamek and N. O'Connor, "A multiscale representation method for nonrigid shapes with a single closed contour," *IEEE Trans. Circuits Syst. Video Technol.*, vol. 14, no. 5, pp. 742–753, May 2004.
- [16] A. R. Backes, D. Casanova, and O. M. Bruno, "A complex network-based approach for boundary shape analysis," *Pattern Recognit.*, vol. 42, no. 1, pp. 54–67, Jan. 2009.
- [17] A. R. Backes and O. M. Bruno, "Shape classification using complex network and multi-scale fractal dimension," *Pattern Recognit. Lett.*, vol. 31, no. 1, pp. 44–51, Jan. 2010.
- [18] K. J. Gaston and M. A. O'Neill, "Automated species identification: Why not?" *Philosoph. Trans. Royal Soc. London, Ser. B*, vol. 359, no. 1444, pp. 655–667, Apr. 2004.
- [19] O. J. O. Soderkvist, "Computer vision classification of leaves from Swedish trees," M.S. thesis, Dept. Electron. Eng., Linköping Univ., Linköping, Sweden, 2001.
- [20] *Intelligent Computing Laboratory (ICL) Plant Leaf Dataset* [Online]. Available: <http://www.intelengine.cn/English/dataset/index.html>
- [21] H. Ling and K. Okada, "An efficient earth mover's distance algorithm for robust histogram comparison," *IEEE Trans. Pattern Anal. Mach. Intell.*, vol. 29, no. 5, pp. 840–853, May 2007.
- [22] J. Wu and J. M. Rehg, "Where am I: Place instance and category recognition using spatial PACT," in *Proc. IEEE Conf. Comput. Vis. Pattern Recognit.*, Anchorage, AK, Jun. 2008, pp. 1–8.
- [23] M. A. Turk and A. P. Pentland, "Face recognition using eigenfaces," in *Proc. IEEE Conf. Comput. Vis. Pattern Recognit.*, Jun. 1991, pp. 586–591.
- [24] P. N. Belhumeur, J. P. Hespanha, and D. J. Kriegman, "Eigenfaces vs. fisherfaces recognition using class specific linear projection," *IEEE Trans. Pattern Anal. Mach. Intell.*, vol. 19, no. 7, pp. 711–720, Jul. 1997.
- [25] Y. Jia, F. Nie, and C. Zhang, "Trace ratio problem revisited," *IEEE Trans. Neural Netw.*, vol. 20, no. 4, pp. 729–735, Apr. 2009.
- [26] H. Li, T. Jiang, and K. Zhang, "Efficient and robust feature extraction by maximum margin criterion," *IEEE Trans. Neural Netw.*, vol. 17, no. 1, pp. 157–165, Jan. 2006.

Detail-Enhanced Exposure Fusion

Zheng Guo Li, *Senior Member, IEEE*,
Jing Hong Zheng, *Member, IEEE*,
and Susanto Rahardja, *Fellow, IEEE*

Abstract—In a typical processing chain of image enhancement, an exposure fusion scheme can be used to synthesize a more detailed low dynamic range (LDR) image directly from a set of differently exposed LDR images, without generation of an intermediate high dynamic range image. In this brief, we introduce a new quadratic optimization-based method to extract fine details from a vector field. The new method extracts fine details from a set of differently exposed LDR images simultaneously. The extracted fine details are then added to an intermediate LDR image which is fused by simply using an existing exposure fusion scheme. With this, the proposed scheme can enhance fine details to produce sharper images.

Index Terms—Detail enhancement, details extraction, exposure fusion, quadratic optimization, vector field.

I. INTRODUCTION

One of the challenges in digital image processing research is the rendering of a high dynamic range (HDR) natural scene on a conventional low dynamic range (LDR) display [1]. This challenge can be addressed by capturing multiple LDR images at different exposure levels. Each LDR image only records a small portion of the dynamic range and partial scene details but the whole set of LDR images collectively contain all scene details. There are two different

Manuscript received January 26, 2012; revised June 6, 2012; accepted June 14, 2012. Date of publication July 10, 2012; date of current version October 12, 2012. The associate editor coordinating the review of this manuscript and approving it for publication was Prof. Zhou Wang.

The authors are with the Signal Processing Department, Institute for Infocomm Research, Agency for Science, Technology, and Research, 138632, Singapore (e-mail: ezgli@i2r.a-star.edu.sg; jzheng@i2r.a-star.edu.sg; rsusanto@i2r.a-star.edu.sg).

Color versions of one or more of the figures in this paper are available online at <http://ieeexplore.ieee.org>.

Digital Object Identifier 10.1109/TIP.2012.2207396

methods to synthesize a more detailed and natural image from the differently exposed LDR images. One is called HDR imaging. An HDR image is first synthesized to include details of all input images [1], [2]. It is then converted into an LDR image by using tone mapping algorithm [3] so as to visualize the HDR scene by conventional display device. The other is called exposure fusion. An LDR image is directly synthesized from all LDR images without generation of an intermediate HDR image [4].

There are both multiple-scale and single scale exposure fusion schemes. Three quality measures of proper exposure, good contrast, and high saturation were used in [4] to determine how much a given pixel will contribute to the final synthesized image. All input images were scaled into several down-sampled layers by using the Laplacian pyramid [5]. The multi-resolution blending preserves the global contrast and ensures that transitions between regions where different images contribute more heavily are difficult to perceive. The exposure fusion scheme in [6] was based on an observation that gradient magnitude becomes larger when a pixel gets a state of better exposed and it decreases gradually as the pixel approaches over/under-exposure. Same as [4], all input images were blended at multiple scales using the pyramidal image decomposition. Recently, several single scale exposure fusion schemes were proposed in [7]–[9]. Different optimization problems are formulated in [7]–[9] with optimal variables as pixel values of the final synthesized image or weights of input images. The final synthesized image can be obtained by solving these optimization problems. As shown in [4], [6]–[9], an exposure fusion scheme neither requires lighting conditions of all input images to be the same nor requires knowledge of exposure times as required by an HDR imaging scheme. It can also synthesize a more detailed LDR image directly from all input images without generation of an intermediate HDR image. However, there is no fine detail enhancement step in existing exposure fusion schemes while fine details can be enhanced by existing tone mapping schemes [3], [10]. It is thus desired to provide a new method for the extraction of fine details from a set of images such that the exposure fusion can enhance fine details as the HDR imaging.

In this brief, a detail-enhanced exposure fusion scheme is proposed. Inspired by existing tone mapping schemes in [3], [10] and detail enhancement schemes via multi-light images in [11], [12], the proposed detail-enhanced exposure fusion scheme includes synthesis of an intermediate image and extraction of fine details from differently exposed images. The final image is generated by integrating the intermediate image with the extracted details. The exposure fusion scheme in [4] is adopted to synthesize an intermediate image and this brief focuses on extraction of fine details. Instead of first extracting fine details from each image and then combining fine details from all images to form the final fine details as in [11] or including all detail information in an auxiliary image [12], the proposed scheme includes a unique method to extract fine details from differently exposed images simultaneously. The proposed method is based on a simple quadratic optimization problem in gradient domain. Input of the quadratic optimization problem is a vector field and output is an image which includes desired fine details. This is different from the optimization problem in [10] with the input as an image. In addition, the new method can extract fine details from a set of images simultaneously, and it is simpler than the methods in [10], [12]. The extracted details are then added to an intermediate image that is fused by using the exposure fusion scheme in [4]. As such, the proposed exposure fusion scheme can enhance fine details to produce sharper images as existing HDR imaging schemes [3], [10]. It is worth noting that a similar method was provided in [13] to enhance fine details via multi-light images, and existing techniques that aim

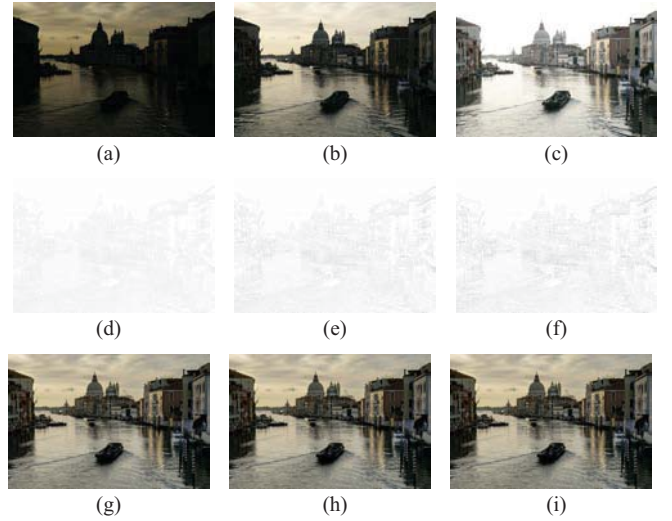


Fig. 1. Comparison of different selections of λ . The input images are captured under the same lighting conditions. Image courtesy of Jacques Joffre. (a) First input image. (b) Second input image. (c) Third input image. (d) Details extracted by $\lambda = 0.25$. (e) Details extracted by $\lambda = 1$. (f) Details extracted by $\lambda = 4$. (g) Final image obtained by $\lambda = 0.25$. (h) Final image obtained by $\lambda = 1$. (i) Final image obtained by $\lambda = 4$.

to enhance fine details in a single image such as unsharp masking might be applicable to the intermediate image.

The rest of this brief is organized as follows. The proposed detail-enhanced exposure fusion scheme is provided in Section II. Experimental results are presented in Section III to verify the performance of the proposed scheme. Finally, concluding remarks are provided in Section IV.

II. DETAIL-ENHANCED FUSION OF DIFFERENTLY EXPOSED IMAGES

In this section, a detail-enhanced exposure fusion scheme is proposed. The proposed scheme first simultaneously extracts fine details from all input images by solving a quadratic optimization problem. An intermediate image is then fused by using the exposure fusion scheme in [4]. The extracted details are finally added to the intermediate image so as to generate the output image.

Let input images be denoted as $Z_k(i, j)$ ($1 \leq k \leq N$) and their luma components denoted as $Y_k(i, j)$ ($1 \leq k \leq N$). The gradient field of $Y_k(i, j)$ ($1 \leq k \leq N$), $(\nabla Y_{k,1}(i, j), \nabla Y_{k,2}(i, j))$ is defined as $(Y_k(i, j+1) - Y_k(i, j), Y_k(i+1, j) - Y_k(i, j))$. Normally, the gradient of a pixel with the largest absolute value among different exposures corresponds to the most desirable detail at a position. However, there is a high likelihood that the maximum gradient is noisy, especially in dark regions of an HDR scene. A vector field is thus constructed by using a weighted average of gradients over all exposures

As indicated in [1], [4], [6], a well exposed pixel includes more reliable information than an under/over-exposed pixel. Therefore, weighting factor of a well exposed pixel is larger than that of an under/over-exposed pixel. Such a weighting function $w(z)$ is defined as [1]

$$w(z) = \begin{cases} z + 1; & \text{if } z \leq 127 \\ 256 - z; & \text{otherwise.} \end{cases} \quad (1)$$

Two weighting factors of a gradient vector $(\nabla Y_{k,1}(i, j), \nabla Y_{k,2}(i, j))$ are computed as

$$W_{k,1}(i, j) = w(Y_k(i, j))w(Y_k(i, j+1)), \quad (2)$$

$$W_{k,2}(i, j) = w(Y_k(i, j))w(Y_k(i+1, j)). \quad (3)$$



Fig. 2. Comparison of the proposed exposure fusion scheme with two multiple-scale exposure fusion schemes in [4] and [6]. Image courtesy of Laurance Meylan. (a) First input image. (b) Second input image. (c) Third input image. (d) Fourth input image. (e) Fifth input image. (f) Sixth input image. (g) Seventh input image. (h) Final image obtained by the exposure fusion scheme in [4]. (i) Final image obtained by the proposed fusion algorithm. (j) Final image obtained by the exposure fusion scheme in [6].

The logarithmic conversion allow us to measure local **contrast** by using spatial difference [11]. The desired **vector field** $\vec{v}(i, j) = (v_1(i, j), v_2(i, j))^T$ is thus computed in *log* domain. Let \mathbf{v}_q , $\mathbf{W}_{k,q}$, and $\mathbf{Y}_{k,q}$ be vectors containing all $v_q(i, j)$'s, $W_{k,q}(i, j)$'s, and $Y_{k,q}(i, j)$'s respectively. The desired vector field is computed as

$$\mathbf{v}_q = \frac{\sum_{k=1}^N \mathbf{W}_{k,q} \nabla \log(\mathbf{Y}_{k,q})}{\sum_{k=1}^N \mathbf{W}_{k,q}}, \quad q = 1, 2. \quad (4)$$

A new quadratic optimization problem is formulated for the extraction of fine details from the vector field $(\mathbf{v}_1, \mathbf{v}_2)$ as follows:

$$\min_{\mathbf{L}_d} \left[\|\mathbf{L}_d\|_2^2 + \lambda \left(\left\| \frac{\mathbf{v}_1 - \frac{\partial \mathbf{L}_d}{\partial x}}{\psi(\mathbf{v}_1)} \right\|_2^2 + \left\| \frac{\mathbf{v}_2 - \frac{\partial \mathbf{L}_d}{\partial y}}{\psi(\mathbf{v}_2)} \right\|_2^2 \right) \right] \quad (5)$$

where $\|\cdot\|_2$ is the l_2 norm. $L_d(i, j)$ represents fine details to be extracted at position (i, j) and \mathbf{L}_d is a vector containing all $L_d(i, j)$'s. The function $\psi(z)$ is selected as [10]

$$\psi(z) = \sqrt{|z|^\gamma + \epsilon} \quad (6)$$

the exponent γ determines the sensitivity to the vector field $(\mathbf{v}_1, \mathbf{v}_2)$. The values of γ in the range of $(1, \infty)$ lead to sparse priors and natural images usually correspond to γ in the range of $[1.2, 1.5]$ [10]. ϵ is a small constant that prevents division by zero in areas where values of $(v_1(i, j), v_2(i, j))$ are zeros. The default values of γ and ϵ are 1.2 and 10^{-4} , respectively. The functions of $\psi(\mathbf{v}_1)$ and $\psi(\mathbf{v}_2)$ are to preserve fine details in \mathbf{L}_d and to prevent sharp edges from \mathbf{L}_d .

There are two terms in the proposed optimization problem (5). The first term is on energy of the details signal which requires that the details signal has small energy. Since the fine details are extracted in *log* domain, the values of all $L_d(i, j)$'s are required to be around zero. The second term is a quadratic function of $(\frac{\partial \mathbf{L}_d}{\partial x} - \mathbf{v}_1)$ and $(\frac{\partial \mathbf{L}_d}{\partial y} - \mathbf{v}_2)$. Its major function is to measure fidelity of $\nabla \mathbf{L}_d$ with respect to \vec{v} . A regularization factor λ is adopted to obtain a tradeoff between these two terms. Increasing the value of λ results in more fine details in \mathbf{L}_d . The value of λ is selected as 1 if not specified. Due to first term of $\|\mathbf{L}_d\|_2^2$, this new optimization problem is different from the optimization problem in [14] even though both of them are in gradient domain.

The optimal solution can be obtained by solving the following equation:

$$\begin{aligned} (I + D_x^T A(\mathbf{v}_1) D_x + D_y^T A(\mathbf{v}_2) D_y) \mathbf{L}_d \\ = D_x^T A(\mathbf{v}_1) \mathbf{v}_1 + D_y^T A(\mathbf{v}_2) \mathbf{v}_2 \end{aligned} \quad (7)$$

where I is the identity matrix, D_x and D_y are discrete differentiation operators, and $A(\mathbf{v}_1)$ and $A(\mathbf{v}_2)$ are $\text{diag}(\frac{1}{\psi(v_1(i, j))})$ and $\text{diag}(\frac{1}{\psi(v_2(i, j))})$, respectively.

Since $(I + D_x^T A(\mathbf{v}_1) D_x + D_y^T A(\mathbf{v}_2) D_y)$ is a sparse and symmetric positive-definite matrix, it is easy to solve for \mathbf{L}_d by using an iterative method with an initialization of 0. An optimal solution can always be obtained for any given guidance field $\vec{v}(i, j)$.

Let an intermediate image that is fused via the scheme in [4] be denoted as $Z_{int}(i, j)$ and it is obtained by a weighted blending of all input images. $C_k(i, j)$, $S_k(i, j)$, and $E_k(i, j)$ measure **contrast**, color saturation, and well-exposedness of pixel $Z_k(i, j)$, respectively. $C_k(i, j)$ is obtained by applying a Laplacian filter to the gray-scale version of each image. $S_k(i, j)$ is computed as the **standard deviation** within the R, G and B channel. $E_k(i, j)$ is yielded by applying a **Gauss curve** to each channel separately and multiplying the results. Their product is denoted as $\tilde{W}_k(i, j)$. $L\{Z_k(i, j)\}^l$ and $G\{\tilde{W}_k(i, j)\}^l$ are Laplacian pyramid of image $Z_k(i, j)$ and Gaussian pyramid of weight map $\tilde{W}_k(i, j)$, respectively. Pixel intensities in the different pyramid levels are blended as

$$L\{\tilde{Z}(i, j)\}^l = \sum_{k=1}^N [L\{Z_k(i, j)\}^l G\{\tilde{W}_k(i, j)\}^l]. \quad (8)$$

The pyramid $L\{\tilde{Z}(i, j)\}^l$ is collapsed to produce an intermediate image $Z_{int}(i, j)$. Similar to tone mapping schemes in [10] and detail enhancement scheme via multi-light images in [11], [12], the final image is synthesized by integrating the intermediate image $Z_{int}(i, j)$ with the extracted details $L_d(i, j)$ as

$$Z_f(i, j) = Z_{int}(i, j) \exp(L_d(i, j)). \quad (9)$$

III. EXPERIMENTAL RESULTS

Due to the space limitation, the proposed scheme is not compared with single scale exposure fusion schemes in [7]–[9] but with two

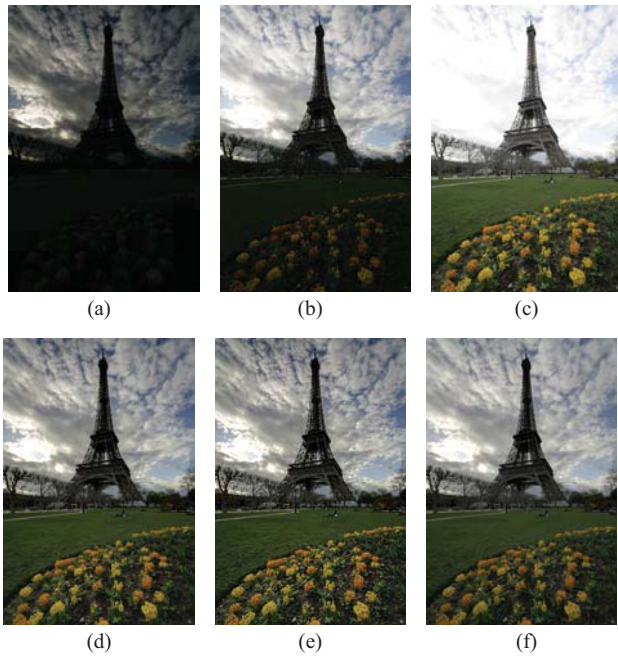


Fig. 3. Comparison of the proposed exposure fusion scheme with two multiple-scale exposure fusion schemes in [4] and [6]. Image courtesy of Jacques Joffre. (a) First input image. (b) Second input image. (c) Third input image. (d) Final image obtained by the exposure fusion scheme in [4]. (e) Final image obtained by the proposed exposure fusion scheme. (f) Final image obtained by the exposure fusion scheme in [6].

multiple-scale exposure fusion schemes in [4], [6] and the the HDR imaging scheme in Photoshop CS5. Five sets of differently exposed LDR images are tested. Three of them are captured under the same lighting conditions and two of them are captured under different lighting conditions. Readers are invited to view the electronic version of the full-size figures in order to better appreciate the differences among images.

The first set of images which is captured under the same lighting conditions is used to test different selections of λ . It is shown in Figure 1 that increasing the value of λ usually results in more fine details in L_d as well as in the final image.

Two sets of images which are also captured under the same lighting conditions are then tested to compare the proposed exposure fusion scheme with the exposure fusion schemes in [4], [6]. The proposed scheme first extracts fine details from all input images and then adds the extracted details to images that are fused by using the schemes in [4], [6]. It thus produces sharper images than the exposure fusion schemes in [4], [6] as demonstrated in Figures 2 and 3. Even though no experimental result is provided by using dynamic range independent objective quality assessment in [15], it was shown in [8] that the exposure fusion scheme in [4] usually causes the loss of visible contrast. With the proposed fine detail enhancement scheme, objective quality assessment results can be expected to be improved.

Finally, two sets of images which are captured under different lighting conditions are used to compare the HDR imaging scheme in Photoshop CS5 with the proposed exposure fusion scheme and the exposure fusion scheme in [4]. One set is composed of a pair of flash and non-flash images as shown in Figures 4(a) and 4(b). The other consists of three images that are captured under different lighting conditions. There is only one lighting resource in Figure 5(a) while there are two and three lighting resources in Figures 5(b) and 5(c), respectively. It is shown in Figures 4(d) and 5(d) that there are artifacts in the final images by using the HDR imaging scheme in

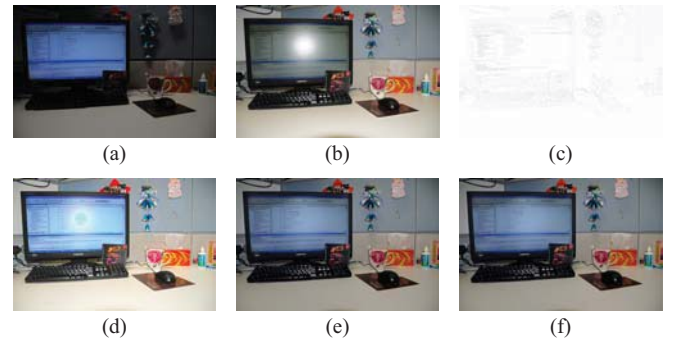


Fig. 4. Comparison of the proposed exposure fusion scheme with the HDR imaging scheme of Photoshop CS5 and the exposure fusion scheme in [4]. (a) Input image without flash. (b) Input image with flash. (c) Details extracted by the proposed exposure fusion scheme. (d) Final image obtained by the HDR imaging scheme in Photoshop CS5. (e) Final image obtained by the proposed exposure fusion scheme. (f) Final image obtained by the exposure fusion scheme in [4].

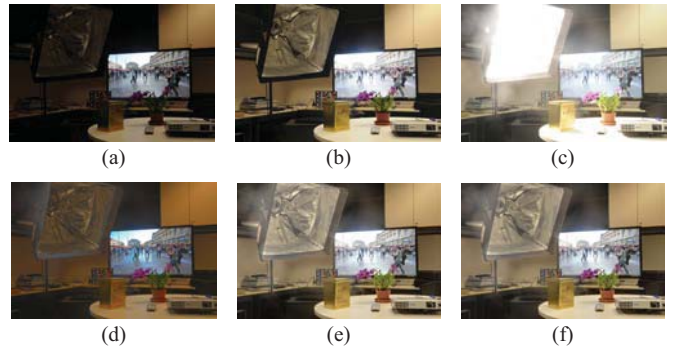


Fig. 5. Comparison of the proposed exposure fusion scheme with the HDR imaging schemes of Photoshop CS5 and the exposure fusion scheme in [4]. (a) Input image with one lighting resource. (b) Input image with two lighting resources. (c) Input image with three lighting resources. (d) Final image obtained by the HDR imaging scheme in Photoshop CS5. (e) Final image obtained by the proposed exposure fusion scheme. (f) Final image obtained by the exposure fusion scheme in [4].


Photoshop CS 5 while there is no artifact by using both the proposed exposure fusions scheme and the exposure fusion scheme in [4]. On the other hand, it is illustrated in Figures 4 and 5 that color saturation is sometimes reduced by using both the proposed exposure fusion scheme and the exposure fusion scheme in [4] even though a color saturation measure is explicitly used in both of them. This problem could be addressed by enhancing the colorfulness of the final image in future research.

IV. CONCLUSION

In this brief, a detail-enhanced exposure fusion scheme has been proposed for the synthesis of a low dynamic range (LDR) image from a set of differently exposed LDR images. The proposed scheme includes a unique method for the simultaneous extraction of fine details from all input images. As a result, it can enhance fine details to produce sharper images as existing high dynamic range imaging schemes.

REFERENCES

- [1] P. E. Debevec and J. Malik, "Rendering high dynamic range radiance maps from photographs," *ACM Trans. Graphics*, vol. 16, no. 3, pp. 369–378, Aug. 1997.
- [2] T. Jinno and M. Okuda, "Multiple exposure fusion for high dynamic range image acquisition," *IEEE Trans. Image Process.*, vol. 21, no. 1, pp. 358–365, Jan. 2012.

- [3] E. Reinhard, G. Ward, S. Pattanaik, and P. E. Debevec, *High Dynamic Range Imaging: Acquisition, Display and Image-Based Lighting*. San Mateo, CA: Morgan Kaufmann, 2005.
- [4] T. Mertens, J. Kautz, and F. V. Reeth, "Exposure fusion: A simple and practical alternative to high dynamic range photography," *Comput. Graphics Forum*, vol. 28, no. 1, pp. 161–171, Jan. 2009.
- [5] P. Burt and T. Adelson, "The Laplacian pyramid as a compact image code," *IEEE Trans. Commun.*, vol. 31, no. 4, pp. 532–540, Apr. 1983.
-  [6] W. Zhang and W. K. Cham, "Gradient-directed multiexposure composition," *IEEE Trans. Image Process.*, vol. 21, no. 4, pp. 2318–2323, Apr. 2012.
- [7] R. Shen, I. Cheng, J. Shi, and A. Basu, "Generalized random walks for fusion of multi-exposure images," *IEEE Trans. Image Process.*, vol. 20, no. 12, pp. 3634–3646, Dec. 2011.
- [8] M. Song, D. Tao, C. Chen, J. Bu, J. Luo, and C. Zhang, "Probabilistic exposure fusion," *IEEE Trans. Image Process.*, vol. 21, no. 1, pp. 341–357, Jan. 2012.
- [9] K. Kotwal and S. Chaudhuri, "An optimization-based approach to fusion of multi-exposure, low dynamic range images," in *Proc. 14th Int. Conf. Inform. Fusion*, Jul. 2011, pp. 1–7.
- [10] Z. Farbman, R. Fattal, D. Lischinski, and R. Szeliski, "Edge-preserving decompositions for multi-scale tone and details manipulation," *ACM Trans. Graphics*, vol. 27, no. 3, pp. 249–256, Aug. 2008.
- [11] R. Fattal, M. Agrawala, and S. Rusinkiewicz, "Multiscale shape and details enhancement for multi-light image collections," *ACM Trans. Graphics*, vol. 26, no. 3, pp. 5101–5110, Aug. 2007.
- [12] J. H. Zheng, Z. G. Li, S. Rahardja, S. S. Yao, and W. Yao, "Collaborative image processing algorithm for details refinement and enhancement via multi-light images," in *Proc. IEEE Int. Acoust. Speech Signal Process. Conf.*, Mar. 2010, pp. 1382–1385.
- [13] Z. G. Li, J. H. Zheng, C. H. Yeo, and S. Rahardja, "Quadratic optimization based small scale details extraction," in *Proc. IEEE Int. Conf. Acoust. Speech Signal Process.*, May 2011, pp. 1309–1312.
- [14] R. Fattal, D. Lischinski, and M. Werman, "Gradient domain high dynamic range compression," *ACM Trans. Graphics*, vol. 21, no. 3, pp. 6701–6710, Aug. 2002.
- [15] T. O. Aydin, R. Mantiuk, K. Myszkowski, and H. P. Seidel, "Dynamic range independent image quality assessment," *ACM Trans. Graphics*, vol. 27, no. 3, pp. 1–10, Aug. 2008.